Analysis of the Lattice Boltzmann Method by the Truncated Moment System

Pietro Asinari, PhD

Department of Energetics, Politecnico di Torino, Torino 10129, Italy,
pietro.asinari@polito.it
http://staff.polito.it/pietro.asinari

Lab for Simulation,
Department of Microsystems Engineering (IMTEK),
University of Freiburg, Freiburg, Germany
29 – 30 September 2008, Black Forest

Outline of this talk

Outline Compass

1. Introduction
   - Lattice Boltzmann Method (LBM)
   - Is it worth the effort?
2. Analysis of the Lattice Boltzmann Method
   - Discrete velocity model on D2Q9 lattice
   - Relevant dimensionless numbers
   - Raw moments and equilibrium
   - Central moments and “cascaded” MRT
   - Truncated moment system
   - Recovering Navier–Stokes
3. Engineering Applications
   - Solid Oxide Fuel Cells (SOFC)

Mesoscopic numerical methods

- Mesoscopic methods (or particle-based methods) try to fill the gap between the microscopic and macroscopic descriptions of the fluid dynamics in multi-scale and multi-physics problems
- Notable examples include:
  - the Lattice Gas Cellular Automata (LGCA)
  - the Lattice Boltzmann Method (LBM)
  - the Discrete Velocity Models (DVM)
  - the Gas Kinetic Scheme (GKS)
  - the Smoothed Particle Hydrodynamics (SPH)
  - the Dissipative Particle Dynamics (DPD)
- Two main categories exist:
  - Primitive Methods (for example GKS) → the kinetic expressions are used for physically–based macroscopic averaging
  - Kinetic Methods (for example LBM) → they may catch truly kinetic physics, if large stencil and proper equilibrium are adopted

Lattice Boltzmann Method (LBM) in a nutshell

- Number of papers on International Journals: 2,000 in the period 1988-2007 (comparison: 10,000 papers on "‘ITER Fusion Project"’ and 28,000 papers on "‘Energy Saving"’)
- Number of books: 14 in the period 2000-2007
- Patents: computational modeling and bio–fluidics
- Industrial sector: automotive
- International conferences:
  - International Conference on Mesoscopic Methods in Engineering and Science, ICMMES
  - Discrete Simulation of Fluid Dynamics in Complex Systems, DSFD

Where the investment is worth: automotive sector

- PowerFLOW® by EXA Corporation, formerly spin–off of MIT: EXA has sustained a greater than 40% annual growth rate in revenues since 2001 (EXA's web site)
- Applications: low–Mach number external aerodynamics, under–hood thermal analysis and low–frequency aeroacoustics (typically up to 500 Hz)
- Advantages: very–user friendly mesh generation (it can handle rough meshes) and good comparison with experimental data by wind tunnel (industrial customers)
- Disadvantages: large hardware requirements and high cost
- Some customers: BMW, Audi, Fiat (Elasis),...

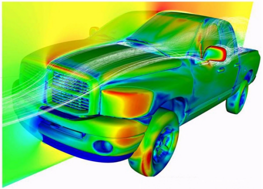

Up to now, we mainly played billiards...

Most of LBM models points to kinetic equations in order to solve fluidynamic equations in continuum regime, i.e. Navier-Stokes (NS).

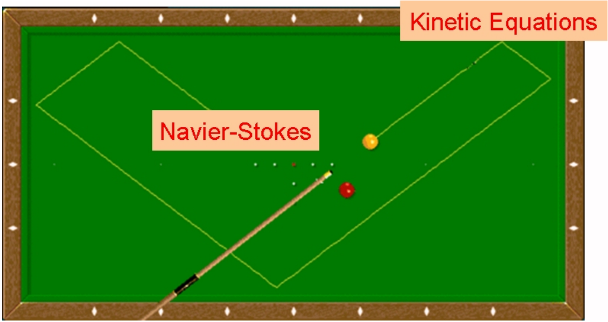

Since the advantage over traditional CFD is thin, LBM should focus more on the truly kinetic content, in order to try to achieve challenging goals in micro–fluidics, with reasonable computational demand.

Where the investment may be worth: micro–fluidics

1. The main challenge is to define a set of generalized gas dynamic equations, which are suitable for microflows and applications.
2. From the kinetic point of view, this means to design a quasi–equilibrium, which is an intermediate state in the path towards the equilibrium, for controlling better the non–equilibrium dynamics. A popular example involves a generalized temperature as a second–order symmetric tensor.
3. Finally, it would be possible to design a Lattice Boltzmann hierarchy of moment equations for solving the previous dynamics. See discussion in Ansumali *et al.* [1].

- One major difficulty is the determination of the boundary condition for the moments because only the lowest few have clear physical meanings.

Outline Compass

Discrete velocity model on D2Q9 lattice

- Let us consider the following discrete velocity model

$$\frac{\partial f}{\partial \tilde{t}} + \tilde{v}_i \frac{\partial f}{\partial \tilde{x}_i} = \frac{Df}{D\tilde{t}} = \tilde{A}(f^{eq} - f), \qquad (1)$$

where $\tilde{v}_i = \tilde{c}\, v_i$ is a list of velocity components, namely

$$v_x = \begin{bmatrix} 0 & 1 & 0 & -1 & 0 & 1 & -1 & -1 & 1 \end{bmatrix}^T, \qquad (2)$$

$$v_y = \begin{bmatrix} 0 & 0 & 1 & 0 & -1 & 1 & 1 & -1 & -1 \end{bmatrix}^T, \qquad (3)$$

f^{eq} and f are lists of discrete populations corresponding to the velocities in the considered lattice and, finally, $\tilde{A}$ is a proper collisional matrix, ruling the relaxation towards the equilibrium.

- The Lagrangian derivative $Df/D\tilde{t}$ can be approximated numerically by the method of characteristics (MOC).
- On a Cartesian homogeneous mesh, the lattice speed $\tilde{c}$ can be tuned such that particles jump to the neighboring nodes according to their discrete microscopic velocity.

Operator splitting → stream & collide paradigm

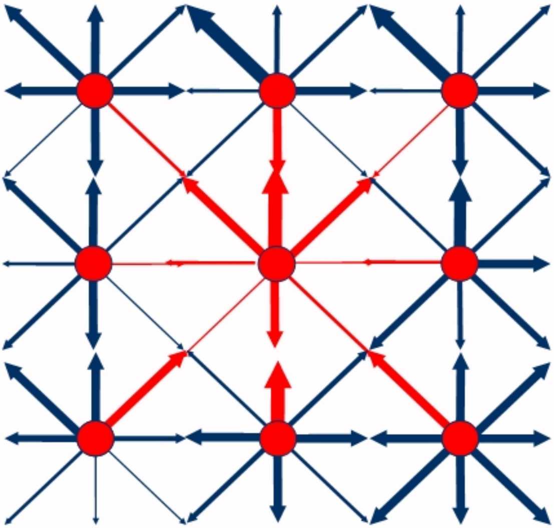

“Faith” is a fine invention, but...

“Faith” is a fine invention
When Gentlemen can see,
But Microscopes are prudent
In an Emergency!

Emily Dickinson
(kinetically interpreted by Stewart Harris)

Our microscope will be the truncated moment system proposed by Asinari and Ohwada [2]

Introducing relevant dimensionless numbers

- Among all the relaxation frequencies, let us define $\tilde{\lambda}_\nu$ that controlling the kinematic viscosity in the continuum limit and $\tilde{\tau} = 1/\tilde{\lambda}_\nu$. Recalling the previous quantities yields

$$\tilde{\tau}\frac{\partial f}{\partial \tilde{t}} + \tilde{\tau}\tilde{c}\, v_i \frac{\partial f}{\partial \tilde{x}_i} = A(f^{eq} - f), \tag{4}$$

where $A = \tilde{A}/\tilde{\lambda}_e^\nu$. Let us introduce the characteristic scales for the flow field, i.e. $\tilde{T}$ and $\tilde{L}$, such that

$$\frac{\partial f}{\partial t} = O(f), \qquad \frac{\partial f}{\partial x_i} = O(f) \tag{5}$$

where $t = \tilde{t}/\tilde{T}$ is the dimensionless time and $x_i = \tilde{x}_i/\tilde{L}$ is the dimensionless space. These assumptions yield

$$\mathrm{Kn}\,\mathrm{Ma}\,\frac{\partial f}{\partial t} + \mathrm{Kn}\, v_i \frac{\partial f}{\partial x_i} = A(f^{eq} - f), \tag{6}$$

where $\mathrm{Kn} = (\tilde{\tau}\tilde{c})/\tilde{L}$, $\mathrm{Ma} = \tilde{U}/\tilde{c}$ and $\tilde{U} = \tilde{L}/\tilde{T}$.

Thinking in terms of moments

- Let us introduce the generic discrete raw moment

$$\bar{r}_{xx\cdots x\,yy\cdots y}(\overbrace{xx\cdots x}^{n\text{ times}},\overbrace{yy\cdots y}^{m\text{ times}}) = \langle v_x^n v_y^m f \rangle. \tag{7}$$

  Examples are: density $\rho = \langle f \rangle$ and momentum $\rho \bar{u}_i = \langle v_i f \rangle$.

- Let us introduce the following set of linearly–independent moments to define the basis of the moment space, namely

$$r = \left[\bar{r}_0, \bar{r}_x, \bar{r}_y, \bar{r}_{xx}, \bar{r}_{yy}, \bar{r}_{xy}, \bar{r}_{xxy}, \bar{r}_{xyy}, \bar{r}_{xxyy}\right]^T. \tag{8}$$

- On the selected lattice, the discrete raw moments r can be computed by means of simple linear combinations of the discrete populations f, namely $r = Mf$ where M is a matrix defined as

$$M = [1, v_x, v_y, v_x^2, v_y^2, v_x v_y, v_x v_y^2, v_x^2 v_y, v_x^2 v_y^2]^T. \tag{9}$$

Local discrete equilibrium

- In the following, we assume $u_i = \tilde{u}_i/\tilde{U}$ and consequently $\bar{u}_i = \text{Ma}\, u_i$. Hence the local discrete equilibrium can be defined (taking advantage of the results for the continuous equilibrium in the infinity velocity space) as $f^{eq} = M^{-1} r^{eq}$, where

$$r^{eq} = \begin{bmatrix} \bar{r}^{eq} \\ \bar{r}_x^{eq} \\ \bar{r}_y^{eq} \\ \bar{r}_{xx}^{eq} \\ \bar{r}_{yy}^{eq} \\ \bar{r}_{xy}^{eq} \\ \bar{r}_{xxy}^{eq} \\ \bar{r}_{xyy}^{eq} \\ \bar{r}_{xxyy}^{eq} \end{bmatrix} = \begin{bmatrix} \rho \\ \text{Ma}\, \rho u_x \\ \text{Ma}\, \rho u_y \\ \rho/3 + \text{Ma}^2\, \rho u_x^2 \\ \rho/3 + \text{Ma}^2\, \rho u_y^2 \\ \text{Ma}^2\, \rho u_x u_y \\ \text{Ma}\, \rho u_y/3 + \text{Ma}^3\, \rho u_x^2 u_y \\ \text{Ma}\, \rho u_x/3 + \text{Ma}^3\, \rho u_x u_y^2 \\ \rho/9 + \text{Ma}^2\, \rho/3(u_x^2 + u_y^2) + \text{Ma}^4\, \rho u_x^2 u_y^2 \end{bmatrix}. \tag{10}$$

Local generalized equilibrium

- What about the relaxation process described by A?
- Not clear yet, because many some degrees of freedom exist. It is better to keep it as much general as possible by defining a local generalized equilibrium $f^{eq*} = f + A(f^{eq} - f)$ such that

$$\mathrm{Kn}\,\mathrm{Ma}\,\frac{\partial f}{\partial t} + \mathrm{Kn}\,v_i \frac{\partial f}{\partial x_i} = A(f^{eq} - f) + f - f = f^{eq*} - f. \qquad (11)$$

- Constraints in the design of the local generalized equilibrium.
  - (consistency) It should recover the desired set of macroscopic equations in the continuum limit
  - (stability) It should be as stable as possible at low viscosities. Not clear (mathematically) how to get this feature (in general) for non–linear equations: need for extensive numerical tests. Physical ideas are very welcome: multiple–relaxation–time (MRT), entropic, “cascaded” MRT,...

Closer look at the “cascaded” MRT

- By realizing the insufficient degree of Galilean invariance of the traditional MRT collision operators, Geier *et al.* [3] proposed to relax differently the central moments, i.e. the moments shifted by the macroscopic velocity, in a moving frame instead of the traditional practice of relaxing the raw moments in the frame at rest, leading to the so-called "cascaded" LBM.
- The "cascaded" LBM uses a generalized local equilibrium in the frame at rest, which depends on both conserved and non–conserved moments, as pointed out in Asinari [4]. This new equilibrium does not affect the consistency of the LBM, but it may enhance the stability of the scheme.

Central moments

- Let us introduce the generic discrete central moment

$$\bar{c}_{xx\cdots x\,yy\cdots y}(\overbrace{xx\cdots x}^{n\text{ times}},\overbrace{yy\cdots y}^{m\text{ times}}) = \langle (v_x - \bar{u}_x)^n (v_y - \bar{u}_y)^m f \rangle, \tag{12}$$

  where the macroscopic velocity components are defined as

$$\bar{u}_x = \langle v_x f \rangle / \langle f \rangle, \qquad \bar{u}_y = \langle v_y f \rangle / \langle f \rangle.$$

- Also in this case

$$c = [\bar{c}_0, \bar{c}_x, \bar{c}_y, \bar{c}_{xx}, \bar{c}_{yy}, \bar{c}_{xy}, \bar{c}_{xxy}, \bar{c}_{xyy}, \bar{c}_{xxyy}]^T . \tag{13}$$

- There is a simple mapping for passing from raw to central moments, e.g.

$$\bar{c}_{xxy} = -\bar{u}_x^2 \bar{u}_y \bar{r}_0 + 2\bar{u}_x \bar{u}_y \bar{r}_x + \bar{u}_x^2 \bar{r}_y - \bar{u}_y \bar{r}_{xx} - 2\bar{u}_x \bar{r}_{xy} + \bar{r}_{xxy}, \tag{14}$$

Central moment calculation

- It is possible to prove that $c = S\, r$, where

$$S(\bar{u}_x, \bar{u}_y) = \begin{bmatrix} 1 & 0 & 0 & 0 & 0 & 0 & 0 & 0 & 0 \\ -\bar{u}_x & 1 & 0 & 0 & 0 & 0 & 0 & 0 & 0 \\ -\bar{u}_y & 0 & 1 & 0 & 0 & 0 & 0 & 0 & 0 \\ \bar{u}_x^2 & -2\bar{u}_x & 0 & 1 & 0 & 0 & 0 & 0 & 0 \\ \bar{u}_y^2 & 0 & -2\bar{u}_y & 0 & 1 & 0 & 0 & 0 & 0 \\ \bar{u}_x\bar{u}_y & -\bar{u}_y & -\bar{u}_x & 0 & 0 & 1 & 0 & 0 & 0 \\ -\bar{u}_x^2\bar{u}_y & 2\bar{u}_x\bar{u}_y & \bar{u}_x^2 & -\bar{u}_y & 0 & -2\bar{u}_x & 1 & 0 & 0 \\ -\bar{u}_x\bar{u}_y^2 & \bar{u}_y^2 & 2\bar{u}_x\bar{u}_y & 0 & -\bar{u}_x & -2\bar{u}_y & 0 & 1 & 0 \\ \bar{u}_x^2\bar{u}_y^2 & -2\bar{u}_x\bar{u}_y^2 & -2\bar{u}_x^2\bar{u}_y & \bar{u}_y^2 & \bar{u}_x^2 & 4\bar{u}_x\bar{u}_y & -2\bar{u}_y & -2\bar{u}_x & 1 \end{bmatrix}. \quad (15)$$

- The previous shift mapping has a very useful property, i.e. $S^{-1}(\bar{u}_x, \bar{u}_y) = S(-\bar{u}_x, -\bar{u}_y)$. This is because the matrix S represents a reversible translation in space.
- The lower triangular structure of the mapping S explains the name “cascaded”.

"Cascaded" MRT

- In the "cascaded" MRT, the collision step is performed in the central moment space. Let us define A such that $A = M^{-1}S^{-1}\Lambda\, SM$, namely

$$f^{eq*} = f + M^{-1}S^{-1}\Omega\, SM\,(f^{eq} - f), \tag{16}$$

where

$$\Omega = \text{diag}\left([0,0,0], \begin{bmatrix} \omega_e^+ & \omega_e^- \\ \omega_e^- & \omega_e^+ \end{bmatrix}, [1, \omega_o, \omega_o, \omega_e]\right), \tag{17}$$

where $\omega_e^+ = (\omega_\xi + 1)/2$, $\omega_e^- = (\omega_\xi - 1)/2$ and $[\omega_\xi,\ \omega_o,\ \omega_e]^T$ are three free tunable parameters, assumed $O(1)$.

- It is possible to prove that, in the continuum limit, the previous choice leads to the kinematic viscosity $\nu = (3\lambda_\nu)^{-1}$ and the second viscosity coefficient $\nu_0 = (3\lambda_\nu\omega_\xi)^{-1} = \nu/\omega_\xi$, where the bulk viscosity is $\xi := \nu_0 - \nu$ in two dimensions.

Usual MRT schematic

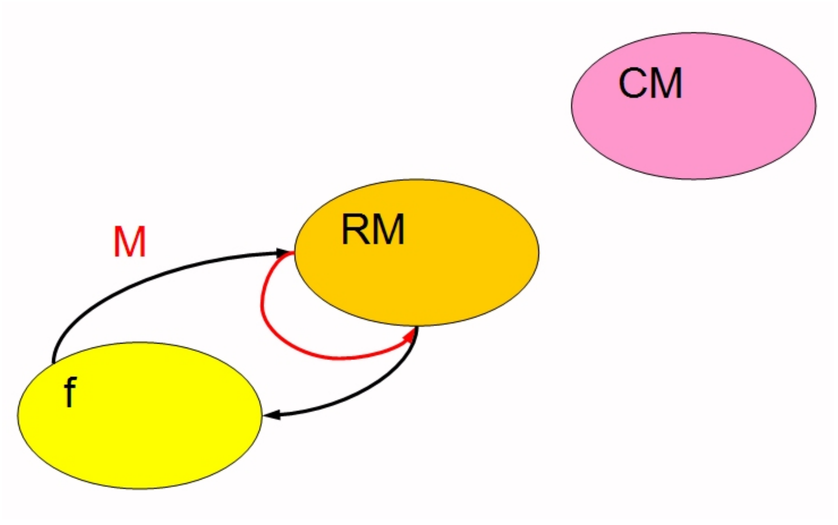

“Cascaded” MRT schematic

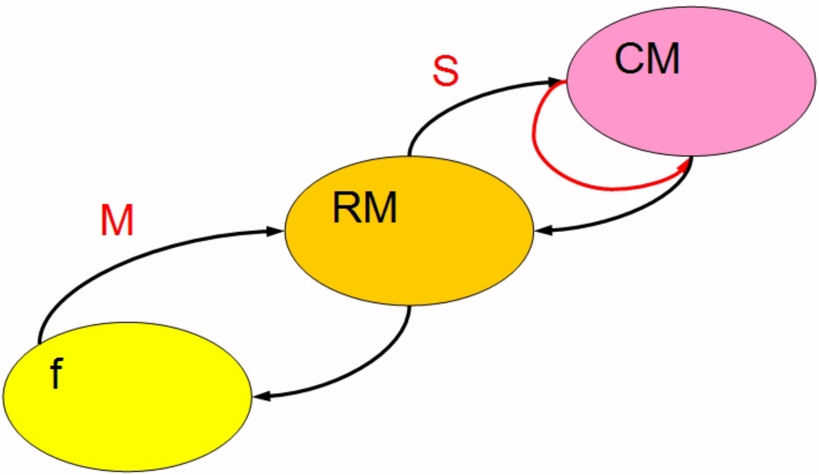

Mass and momentum

- In the following, mass and momentum conservation (no mass sources and no external forces) are assumed.
- The equations for mass and momentum are

$$\frac{\partial \rho}{\partial t} + \frac{\partial (\rho u_i)}{\partial x_i} = 0, \tag{18}$$

$$\mathrm{Ma}^2 \frac{\partial (\rho u_i)}{\partial t} + \frac{\partial \bar{r}_{i\,j}}{\partial x_j} = 0. \tag{19}$$

- Clearly in order to recover Navier–Stokes (NS) system of equations, it must hold $\partial \bar{r}_{i\,j}/\partial x_j \sim \mathrm{Ma}^2$.
- The actual expression of $\bar{r}_{i\,j}$ depends on the dynamics of the higher–order moments. There is a hierarchical system of moment equations.
- The assumption to consider a lattice, i.e. a finite set of Q discrete velocities, is enough to produce a closure in the moment system. In particular, only Q independent moment equations exist.

Stress tensor

- The components of the stress tensor satisfy the following equations

$$\text{Kn}\,\text{Ma}\,\frac{\partial \bar{r}_{xx}}{\partial t} + \text{Kn}\,\text{Ma}\,\frac{\partial (\rho u_x)}{\partial x} + \text{Kn}\,\frac{\partial \bar{r}_{xxy}}{\partial y} = \bar{r}_{xx}^{eq*} - \bar{r}_{xx}, \tag{20}$$

$$\text{Kn}\,\text{Ma}\,\frac{\partial \bar{r}_{yy}}{\partial t} + \text{Kn}\,\frac{\partial \bar{r}_{yyx}}{\partial x} + \text{Kn}\,\text{Ma}\,\frac{\partial (\rho u_y)}{\partial y} = \bar{r}_{yy}^{eq*} - \bar{r}_{yy}, \tag{21}$$

$$\text{Kn}\,\text{Ma}\,\frac{\partial \bar{r}_{xy}}{\partial t} + \text{Kn}\,\frac{\partial \bar{r}_{xxy}}{\partial x} + \text{Kn}\,\frac{\partial \bar{r}_{yyx}}{\partial y} = \bar{r}_{xy}^{eq*} - \bar{r}_{xy}, \tag{22}$$

where

$$\bar{r}_{xx}^{eq*} = \bar{r}_{xx} + \omega_e^{+}(\bar{r}_{xx}^{eq} - \bar{r}_{xx}) + \omega_e^{-}(\bar{r}_{yy}^{eq} - \bar{r}_{yy}), \tag{23}$$

$$\bar{r}_{yy}^{eq*} = \bar{r}_{yy} + \omega_e^{-}(\bar{r}_{xx}^{eq} - \bar{r}_{xx}) + \omega_e^{+}(\bar{r}_{yy}^{eq} - \bar{r}_{yy}), \tag{24}$$

$$\bar{r}_{xy}^{eq*} = \bar{r}_{xy}^{eq}. \tag{25}$$

- The lattice deficiencies show up in the spatial fluxes.

Third–order moments

- Similarly for the third–order moments

$$\text{Kn}\,\text{Ma}\,\frac{\partial \bar{r}_{xxy}}{\partial t} + \text{Kn}\,\frac{\partial \bar{r}_{xy}}{\partial x} + \text{Kn}\,\frac{\partial \bar{r}_{xxyy}}{\partial y} = \bar{r}^{eq*}_{xxy} - \bar{r}_{xxy}, \tag{26}$$

$$\text{Kn}\,\text{Ma}\,\frac{\partial \bar{r}_{yyx}}{\partial t} + \text{Kn}\,\frac{\partial \bar{r}_{xxyy}}{\partial x} + \text{Kn}\,\frac{\partial \bar{r}_{xy}}{\partial y} = \bar{r}^{eq*}_{xyy} - \bar{r}_{xyy}, \tag{27}$$

where

$$\begin{aligned}
\bar{r}^{eq*}_{xxy} \quad - \quad & \bar{r}_{xxy} = \omega_o(\bar{r}^{eq}_{xxy} - \bar{r}_{xxy}) \\
& + \text{Ma}\,(\omega_e^+ - \omega_o) u_y (\bar{r}^{eq}_{xx} - \bar{r}_{xx}) + \text{Ma}\,\omega_e^- u_y (\bar{r}^{eq}_{yy} - \bar{r}_{yy}) \\
& + 2\,\text{Ma}\,(\omega_e - \omega_o) u_x (\bar{r}^{eq}_{xy} - \bar{r}_{xy}),
\end{aligned} \tag{28}$$

$$\begin{aligned}
\bar{r}^{eq*}_{xyy} \quad - \quad & \bar{r}_{xyy} = \omega_o(\bar{r}^{eq}_{xyy} - \bar{r}_{xyy}) \\
& + \text{Ma}\,\omega_e^- u_x (\bar{r}^{eq}_{xx} - \bar{r}_{xx}) + \text{Ma}\,(\omega_e^+ - \omega_o) u_x (\bar{r}^{eq}_{yy} - \bar{r}_{yy}) \\
& + 2\,\text{Ma}\,(\omega_e - \omega_o) u_y (\bar{r}^{eq}_{xy} - \bar{r}_{xy}).
\end{aligned} \tag{29}$$

Continuum limit

- Since we are interested in the continuum limit, i.e. $\text{Kn} \ll 1$, let us search for a simplified expression for the stress tensor, involving only terms $O(\text{Kn}^0)$ and $O(\text{Kn}^1)$.
- Since $\bar{r}_{ij}^{eq} - \bar{r}_{ij} = O(\text{Kn}\,\text{Ma})$, then

$$\bar{r}_{xxy} = \bar{r}_{xxy}^{eq} + O(\text{Kn}\,\text{Ma}^2), \quad (30)$$

$$\bar{r}_{xyy} = \bar{r}_{xyy}^{eq} + O(\text{Kn}\,\text{Ma}^2). \quad (31)$$

- Consequently

$$\bar{r}_{xx}^{eq*} - \bar{r}_{xx} = \text{Kn}\,\text{Ma}\,\frac{\partial \bar{r}_{xx}^{eq}}{\partial t} + \text{Kn}\,\text{Ma}\,\frac{\partial(\rho u_x)}{\partial x} + \text{Kn}\,\frac{\partial \bar{r}_{xxy}^{eq}}{\partial y} + O(\text{Kn}^2\,\text{Ma}^2), \quad (32)$$

$$\bar{r}_{yy}^{eq*} - \bar{r}_{yy} = \text{Kn}\,\text{Ma}\,\frac{\partial \bar{r}_{yy}^{eq}}{\partial t} + \text{Kn}\,\frac{\partial \bar{r}_{yyx}^{eq}}{\partial x} + \text{Kn}\,\text{Ma}\,\frac{\partial(\rho u_y)}{\partial y} + O(\text{Kn}^2\,\text{Ma}^2), \quad (33)$$

$$\bar{r}_{xy}^{eq} - \bar{r}_{xy} = \text{Kn}\,\text{Ma}\,\frac{\partial \bar{r}_{xy}^{eq}}{\partial t} + \text{Kn}\,\frac{\partial \bar{r}_{xxy}^{eq}}{\partial x} + \text{Kn}\,\frac{\partial \bar{r}_{yyx}^{eq}}{\partial y} + O(\text{Kn}^2\,\text{Ma}^2). \quad (34)$$

Low Mach number assumption

- Let us suppose Ma < 1, i.e. Ma has a fixed small value, then

$$\bar{r}_{xx}^{eq*} - \bar{r}_{xx} = \mathrm{Kn}\,\mathrm{Ma}\,\frac{2}{3}\frac{\partial(\rho u_x)}{\partial x} + O(\mathrm{Kn}^2\,\mathrm{Ma}^2) + O(\mathrm{Kn}\,\mathrm{Ma}^3), \qquad (35)$$

$$\bar{r}_{yy}^{eq*} - \bar{r}_{yy} = \mathrm{Kn}\,\mathrm{Ma}\,\frac{2}{3}\frac{\partial(\rho u_y)}{\partial y} + O(\mathrm{Kn}^2\,\mathrm{Ma}^2) + O(\mathrm{Kn}\,\mathrm{Ma}^3), \qquad (36)$$

$$\bar{r}_{xy}^{eq} - \bar{r}_{xy} = \mathrm{Kn}\,\mathrm{Ma}\left[\frac{1}{3}\frac{\partial(\rho u_y)}{\partial x} + \frac{1}{3}\frac{\partial(\rho u_x)}{\partial y}\right] + O(\mathrm{Kn}^2\,\mathrm{Ma}^2) + O(\mathrm{Kn}\,\mathrm{Ma}^3). \qquad (37)$$

Introducing $S_{ij} = \nu\left(\partial_j u_i + \partial_i u_j - \partial_k u_k\right) + \nu_0 \partial_k u_k$ yields

$$\begin{aligned}\bar{r}_{ij}^{eq} - \bar{r}_{ij} &= \mathrm{Kn}\,\mathrm{Ma}\,\rho\,S_{ij} + O(\mathrm{Kn}^2\,\mathrm{Ma}^2) + O(\mathrm{Kn}\,\mathrm{Ma}^3) \\ &+ O(\mathrm{Kn}\,\mathrm{Ma}\,\partial_x\rho) + O(\mathrm{Kn}\,\mathrm{Ma}\,\partial_y\rho). \qquad (38)\end{aligned}$$

- Four errors appear, but only the first is very small.

Recovering Navier–Stokes

- The equations for mass and momentum in the continuum limit are

$$\frac{\partial \rho}{\partial t} + \frac{\partial (\rho u_i)}{\partial x_i} = 0, \tag{39}$$

$$\frac{\partial (\rho u_i)}{\partial t} + \frac{\partial}{\partial x_j}(\rho u_i u_j) + \frac{1}{\mathrm{Ma}^2}\frac{\partial \rho/3}{\partial x_i} = \frac{1}{\mathrm{Re}}\frac{\partial (\rho S_{ij})}{\partial x_j}$$
$$+O(\mathrm{Kn}^2) + O(\mathrm{Kn}\,\mathrm{Ma}) + O(\mathrm{Kn}\,\partial_x \rho/\mathrm{Ma}) + O(\mathrm{Kn}\,\partial_y \rho/\mathrm{Ma}), \tag{40}$$

  where $\mathrm{Re} = \mathrm{Ma}/\mathrm{Kn}$ is the Reynolds number.

- Finally, introducing $p = (\rho - \rho_0)/(3\,\mathrm{Ma}^2)$ yields

$$\frac{\partial (\rho u_i)}{\partial t} + \frac{\partial}{\partial x_j}(\rho u_i u_j) + \frac{\partial p}{\partial x_i} = \frac{1}{\mathrm{Re}}\frac{\partial (\rho S_{ij})}{\partial x_j} + O(\mathrm{Kn}^2) + O(\mathrm{Kn}\,\mathrm{Ma}). \tag{41}$$

Outline Compass

INTESE Laboratory at DENER

- **Activities**
  - **Polarization curves**
  - **Dynamic operation**
  - **Analysis of fuel utilization factor**
  - **Thermal characterization**
  - **Analysis of he effects of materials and production procedures and technologies**
  - **Small stacks**
  - **Analysis of the effects of the microscopic topology of the porous materials on the cell behavior**

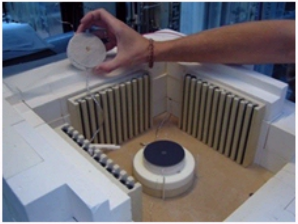

Solid Oxide Fuel Cells (SOFC)

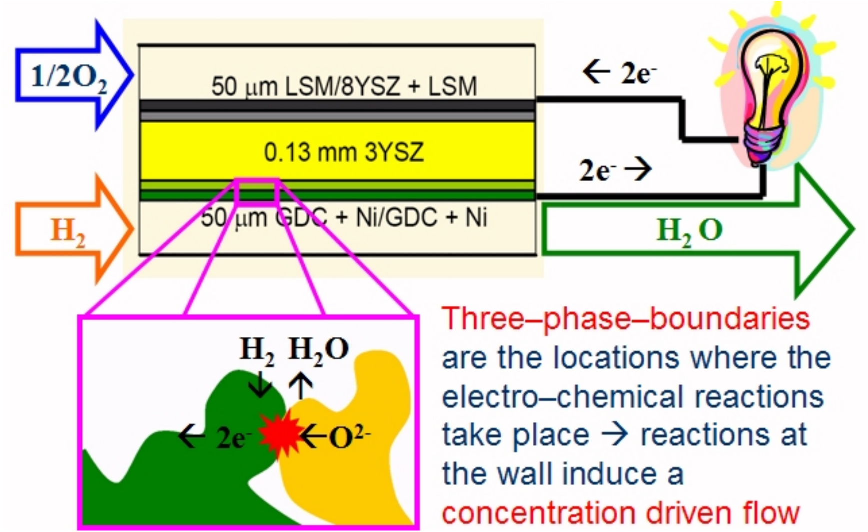

Three–phase–boundaries are the locations where the electro–chemical reactions take place → reactions at the wall induce a concentration driven flow

Reconstructed topology by granulometry law

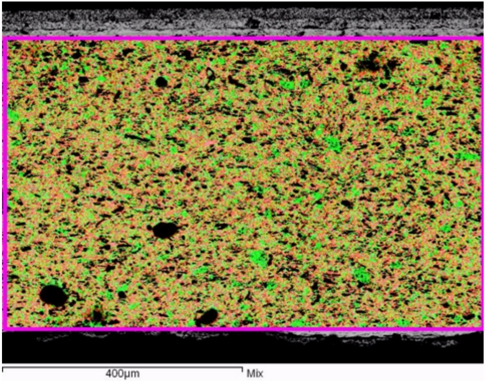

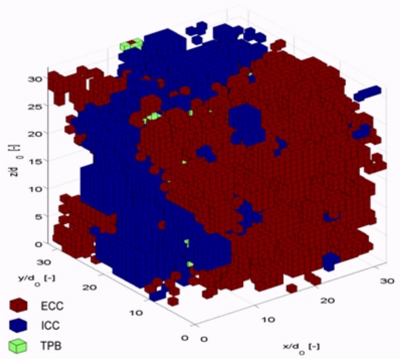

Reconstructed topology by two-point statistics

- 3D reconstructed image obtained by two – point statistics (porosity + autocorrelation) of 2D pictures: kindly provided by dr. B.V. Kasula (Virginia Tech, USA) using IMAGO ® software

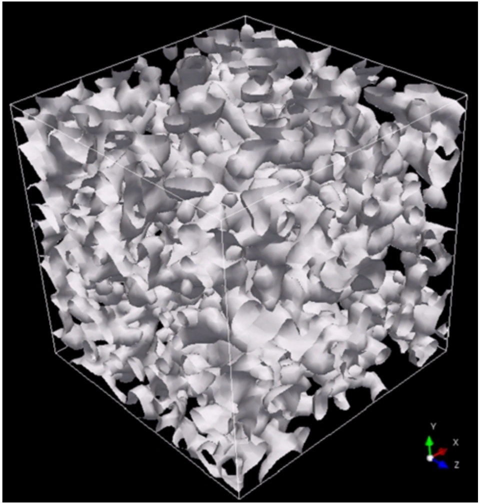

Fluid flow at the gas channel interface

- Hexahedral mesh 256^3=16.7 MCell → 134.2 MDof for binary mixture (H_2O/H_2) in 3D porous medium (Asinari et al., 2007).
- 100,000 collisions.
- Wall clock time 57 hours with a 64 CPU cluster.
- Parallelization efficiency 85 % with non-optimized domain decomposition.

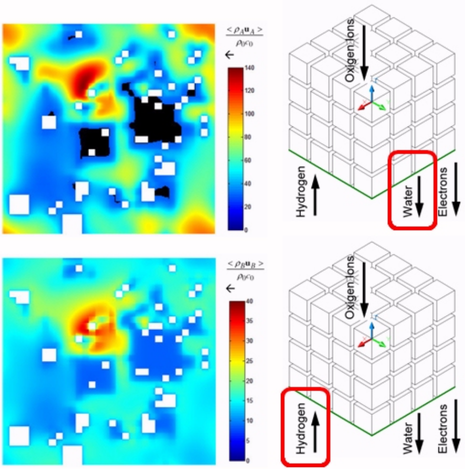

Spatial dependence of tortuosity

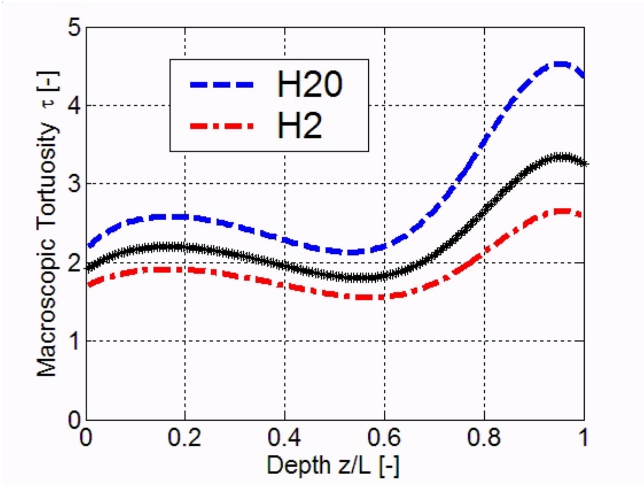

Additional details are reported in Asinari *et al.* [5]

Conclusions

- Concerning the Navier–Stokes solvers, LBM may show some advantages over conventional methods, mainly because of the possibility to deal with quite rough meshes. This may be a feature which is not exclusive of LBM.
- LBM seems to have promising features for catching rarefied effects beyond Navier–Stokes. However this issue has not been proved yet in a completely convincing way.
- The truncated moment system represents a simple tool to analyze LBM schemes: it is exact and it does not require a given scaling of the dimensionless numbers.

References I

[1] S. Ansumali, I. V. Karlin, S. Arcidiacono, A. Abbas, and N. I. Prasianakis.
Hydrodynamics beyond navier-stokes: Exact solution to the Lattice Boltzmann Hierarchy.
Physical Review Letters, 98(12):124502, 2007.

[2] P. Asinari and T. Ohwada.
Equivalence between kinetic method for fluid-dynamic equations and macroscopic finite-difference scheme.
Comput. Math. Appl., 2008.
(in press).

[3] M. Geier, A. Greiner, and J.G. Korvink.
Cascaded digital lattice Boltzmann automata for high reynolds number flow.
Phys. Rev. E, 73(6):66705 – 1, 2006.

[4] P. Asinari.
Generalized local equilibrium in the cascaded lattice Boltzmann method.
Phys. Rev. E, 78:016701 – 1, 2008.

[5] P. Asinari, M.R. von Spakovsky, M.Q. Calì, and B.V. Kasula.
Direct numerical calculation of the kinematic tortuosity of reactive mixture flow in the anode layer of solid oxide fuel cells by the Lattice Boltzmann Method.
J. Power Sources, 170:359–375, 2007.